Article

Sequence stratigraphy and microplankton palaeoenvironmental dynamics across the Jurassic–Cretaceous transition in the Canadian Arctic

Stephen INGRAMS[1]* , David W. JOLLEY[1] and Simon SCHNEIDER[2]

[1] Department of Geology and Geophysics, School of Geosciences, University of Aberdeen, King's College, Aberdeen, AB24 3UE, UK.
[2] Cambridge Arctic Shelf Programme, West Building, Madingley Rise, Madingley Road, Cambridge, CB3 0UD, UK.
*Corresponding author. Email: r01si18@abdn.ac.uk

ABSTRACT: The Jurassic to Cretaceous strata exposed in the Rollrock Section, Sverdrup Basin, Arctic Canada, represent one of the northernmost continuous outcrops spanning this poorly understood transition. The Oxfordian–Valanginian mudstones of the Rollrock Section were deposited in a shallow marine environment and, as such, provide the ideal lithology to investigate the response of high latitude dinoflagellate cyst populations to the frequent environmental perturbations of this time. Using a multivariate statistical approach, distinct palaeoecologically significant groups are identified and directly linked to time and palaeoenvironments, allowing for the reconstruction of underlying long term palaeoenvironmental trends. These palaeoenvironmental trends are identified to be driven by sequence stratigraphic cycles. For the first time, fourth order sequences are recorded from this pivotal period in the Sverdrup Basin and reveal an additional level of short term climatic events that complicate the identification of long term trends. The relationship existing between marine phytoplankton and climate is utilised to decipher the interplay of long-term and short-term climate fluctuations, distinguishing them from evolutionary trends. Two groups of dinoflagellate cysts, identified by process morphology, are recorded to act as environmental proxies. High percentages of proximochorate dinoflagellate cysts, such as *Trichodinium erinaceoides*, indicate more proximal, high energy, nutrient rich conditions and are dominant in fourth order transgressive systems tracts. High percentages of chorate dinoflagellate cysts, such as *Oligosphaeridium complex*, signify distal, low energy, nutrient depleted conditions and are dominant in fourth order highstand systems tracts.

KEY WORDS: Berriasian, palynology, Sverdrup Basin, Tithonian, Valanginian.

1. Introduction

The Jurassic–Cretaceous transition is a known period of significant environmental perturbations, the frequency and magnitude of which remain poorly understood. (Tennant *et al.* 2017 and references within). During the Tithonian and Valanginian two significant sea level falls of ~40 m occurred (Haq 2014), reducing marine connectivity resulting in the establishment of unique bioprovinces reflecting spatial and temporal differences in marine flora and fauna. The intricate relationship between marine phytoplankton and climate allows for the utilisation of dinoflagellate cysts as a palaeoenvironmental proxy (e.g., Dypvik & Harris, 2001; Retallack, 2008; Davies *et al.* 2015), which is used to decipher the interplay of long term and short term climate fluctuations, distinguishing them from evolutionary signals. Dinoflagellate cyst morphological trends are of particular importance across the Jurassic–Cretaceous transition, as a major shift to chorate cysts across the Arctic is observed (e.g., Lebedeva & Nikitenko, 1999; Nøhr-Hansen *et al.* 2019; Sliwińska *et al.* 2020; Ingrams *et al.* 2021).

The Rollrock Section, Arctic Canada, is one of the highest palaeolatitude continuous sections spanning the Jurassic–Cretaceous transition, and the northernmost section in the Sverdrup Basin (Schneider *et al.* 2020; Ingrams *et al.* 2021). Previous palynological studies of assemblages recovered from the basin focused entirely on biostratigraphy (Ingrams *et al.* 2021) and/or had less complete sections, lower sample numbers or more widely spaced samples (Davies 1983; Galloway *et al.* 2013, 2015; Nguyen *et al.* 2020). More recent palynological analysis of the basin has been undertaken on incomplete or slightly more southern sections and focused on terrestrial rather than marine floras (Galloway *et al.* 2013, 2015, 2020). This study combines the results of modern palynological processing techniques with a quantitative multivariate statistical approach, to provide an improved understanding of fluctuating marine floral assemblages and palaeoclimatic trends across the Jurassic–Cretaceous boundary in the Sverdrup Basin. The terrestrial component of the recovered assemblages has been analysed separately (work in progress). Based on the recovered pattern, a framework of third order and fourth order depositional sequences is established for the transition interval.

Continuous exposures across the Jurassic–Cretaceous transition at high palaeo-latitudes is rare (e.g., Jelby *et al.* 2020 and references within). Therefore, the mudstones of the Rollrock
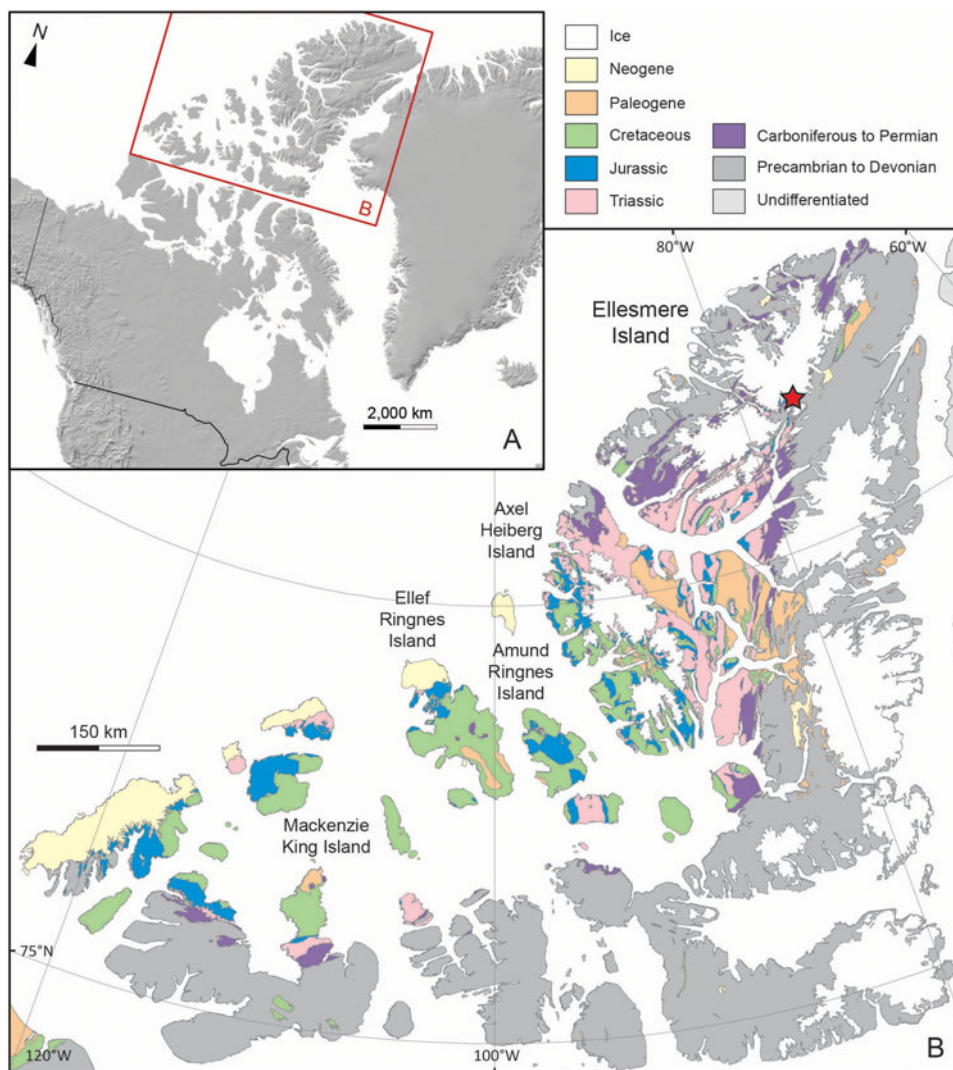
Figure 1 Location map of the Sverdrup Basin (a). Geology of the Sverdrup Basin (after Harrison *et al.* 2011) (b). Location of the Rollrock Section on Ellesmere Island (star), (modified from Schneider *et al.* 2020).

Section provide an ideal archive for palynomorph assemblages from across the Jurassic–Cretaceous transition. Palynomorphs occur continuously over the succession, enabling multivariate quantitative statistical analyses. These analyses in turn provide statistical evidence for environmental controls over marine phytoplankton assemblages.

2. Geological setting

The Sverdrup Basin is located within the Canadian Arctic Islands, encompassing an area of ~300,000 km^2 (Balkwill 1978; Embry & Beauchamp 2019; Fig. 1). Basin development began in the Early Carboniferous on a basement of Neoproterozoic–Devonian sedimentary strata, terminating in the latest Cretaceous with the Eurekan Orogeny (Hadlari *et al.* 2016; Embry & Beauchamp 2019).

Since development began, 13–15 km of sedimentary strata were deposited which have been assigned to eight significant, unconformity-bound phases of deposition (Embry & Beauchamp 2019). The Oxfordian–Valanginian strata studied herein were deposited during the fifth phase (Rhaetian–mid-Valanginian), a period characterised by relatively shallow marine deposition. The sedimentary rocks of the middle and latter portions of this phase (Pliensbachian–mid-Valanginian) were deposited in a syn-rift setting (Hadlari *et al.* 2016), climaxing around the Jurassic–Cretaceous transition, which is the main focus of this study. During

this phase, more distal locations, such as the Rollrock Section, were dominated by mud deposition, with sands representing only the most severe regressive phases.

2.1. Lithostratigraphy
The studied section, initially described by Wilson (1976), crops out on the northern slope of the Rollrock River Valley on Northern Ellesmere Island, extending over 5 km laterally (Fig. 1). The logged and sampled section is a 560 m thick continuous exposure of Late Jurassic–Early Cretaceous sedimentary rock. The base of the logged section is located near 81.61172°N, −75.58489°W with the top near 81.617447°N, −75.596306°W; WGS84 datum (detailed log in Schneider *et al.* 2020). The Rollrock Section begins with the Ringnes Formation, a thick succession of dark, thinly bedded or laminated mudstones and siltstones, with rare intercalations of fine-grained sandstones, becoming more abundant in the uppermost 20 m of the unit. This interval was previously assigned to the Awingak Formation by Embry (in Mayr and Trettin, 1996), but is not sand dominated and thus does not conform to the lithological definition of this unit. Nevertheless, the sandstone horizons are likely a distal representation of the Sildre Member of the Awingak Formation (see Schneider *et al.* 2020 for details). Palynological and macro-fossil investigations give an Oxfordian to (early) Tithonian age for the Ringnes Formation (Schneider *et al.* 2020; Ingrams *et al.* 2021).

At 251 m, there is a sharp contact between the fine-grained sandstones and overlying mudstones. This change in lithology marks the boundary between the Ringnes and Deer Bay formations (Schneider *et al.* 2020). The Deer Bay Formation consists of dark, thinly bedded or laminated mudstones. A sandstone bed containing large concretions at 273 m and a thin indurated siltstone interval are the only interruptions to mudstone deposition. Palynological and macrofossil evidence gives a Tithonian–Valanginian age for the Deer Bay Formation (Schneider *et al.* 2020; Ingrams *et al.* 2021). Eight horizons of glendonites, which have been described as the most distinguishing aspect of the upper Deer Bay Formation by Kemper (1975), have been recorded from the upper part of the Rollrock Section (Schneider *et al.* 2020), and palynological evidence identifies these as Valanginian in age (Ingrams *et al.* 2021).

Beginning at 520 m there are frequent intercalations of siltstone and, very-fine to fine grained sandstone horizons. A clean, trough cross-bedded sandstone occurring at 524.5 m indicates a lithological switch to a sand dominated succession. This change in lithofacies has been interpreted as the boundary between the Deer Bay Formation and the Isachsen Formation (Schneider *et al.* 2020). The latter is generally defined as a succession of light coloured quartzose sandstone and conglomerates, with interbeds of dark siltstone, shale, and coal (e.g., Embry, 1985; Galloway *et al.* 2015). Only one sample was taken from a shale interval in the Isachsen Formation at 537 m and as such, this unit is not the main focus of this study.

2.2. Chronostratigraphy

The study area lacks an accurate geochronostratigraphical framework. Consequently, the ages of the formations have been constrained using a combination of macropalaeontology and palynology (Galloway *et al.* 2015, 2020; Schneider *et al.* 2020; Ingrams *et al.* 2021). Ammonites are the most stratigraphically useful macrofossils, but fossiliferous horizons yield low abundances and are widely spaced across the Jurassic and Cretaceous. Ammonites combined with *Buchia* bivalves have been used to create a chronological framework for the basin (Jeletzky 1984; Schneider *et al.* 2020), which was utilised when examining the distribution of palynomorphs in the Rollrock Section, culminating in a new palynological biostratigraphic scheme for the region (Ingrams *et al.* 2021). The result of these studies is that the Rollrock section is now the stratigraphically best constrained section spanning the Jurassic–Cretaceous transition in the Sverdrup Basin.

3. Dinoflagellate cyst functional morphology

Fossil dinoflagellate cysts have been subdivided into three broad categories defined by process length as a percentage of the shortest diameter of the central body (Sarjeant 1982). By definition, process length in proximate cysts is less than 10%, in proximochorate cysts between 10% and 30%, and in chorate cysts greater than 30%. While this differentiation is arbitrary and cyst placement into these three categories can vary between authors (due to intraspecific variability in process length), it is still useful in palaeoenvironmental interpretations.

Dinoflagellates have evolved three key strategies enabling them to survive: they are good competitors; stress-tolerant; and disturbance-tolerant. This allows them to exist in a wide-ranging variety of aqueous and sea ice environments (Reynolds 1989; Smayda & Reynolds 2001, 2003). Investment in rapid development and reproduction enhances innate competitive ability. Resting cyst stages allow dinoflagellates greater control over when blooming occurs, with cysts remaining docile for up to 10 years if environmental conditions are not adequate for excystment (Smayda 2002). This is one reason dinoflagellates are not

as affected by global extinction events such as the Cretaceous–Palaeogene boundary (e.g., Galeotti *et al.* 2004). Stress tolerance enables species to survive and function in severely nutrient depleted environments, including Arctic environments with highly seasonal climates, where polar winter brings darkness and colder temperatures, resulting in a diminished nutrient supply. Disturbance tolerance allows species to withstand frequent or continuous turbulence in shallow marine environments. These adaptations are not uniform across all dinoflagellate species, as some are able to tolerate higher levels of stress than others (Smayda & Reynolds 2003).

4. Methods

4.1. Study area
All sampled material was collected from the Rollrock Section (Figs 1, 2). Samples were selected from shale beds in the basal 355 m of the section using a combined targeted and systematic approach. However, gaps of no more than 9 m were left unsampled ($n = 90$, AVE = 3.98 m.). The top 168 m yielded higher quality preservation and as such were sampled at 1.5 m density ($n = 109$). Three samples located at 474 m, 502.5 m and 504 m were lost during transport. A single sample was prepared from the overlying Isachsen Formation at 537 m.

4.2. Laboratory processing
Selected samples were prepared using hydrofluoric (HF) and hydrochloric acid (HCl) maceration. 114 samples were prepared by MB Stratigraphy Ltd. and 86 samples were prepared in the University of Aberdeen. Preparations were done concurrently using the same technique outlined below.

Samples were lightly broken apart and then demineralised using HF. HCl was used to remove any carbonates and HF precipitate. The remaining organic component was concentrated by a combination of nitric oxidation (by Schultze solution) and swirling techniques. Where necessary samples were processed in a centrifuge for heavy liquid separation. This was done by the sodium-polytungstate ($3Na_2WO_4·9WO_3$) method with the inorganic compound made up to a specific gravity of 2.2.

The remaining organic component was strewn onto a glass slide and analysed under a microscope. A count of 250 marine palynomorphs was aimed for. In samples with poor recovery, the entire slide was analysed. In samples with recovery greater than 250, the remaining slide was analysed for additional, rare taxa, which were recorded outside of the count.

Portable X-ray fluorescence (PXRF) analysis was undertaken using an Olympus Delta Premium handheld XRF analyser, housed in the University of Aberdeen. Prior to analysis approximately 10–15 g of all samples were ground into a fine powder using a pestle and mortar. The grinding process homogenised the samples creating a flat surface and sufficient depth to enable measurements to be accurately taken. After powdering samples were carefully transferred into a glass vial. The vial lids were removed and replaced by a thin layer of non-polyvinyl chloride cling film. These vials were then inverted and transferred into the Delta PXRF workstation containing the PXRF analyser, taking care to line the analyser aperture up with the centre of the powder to prevent the glass of the vial being analysed.

4.3. Multivariate techniques
Multivariate statistical analyses are based on quantitate data of marine dinoflagellate cysts preserved in the Rollrock Section across the Ringnes, Deer Bay, and Isachsen Formations (Appendix 1 available at https://doi.org/10.1017/tre2200008). The computer software program PAST (Hammer *et al.* 2001; Hammer & Harper 2006) was used for Q-mode hierarchical cluster
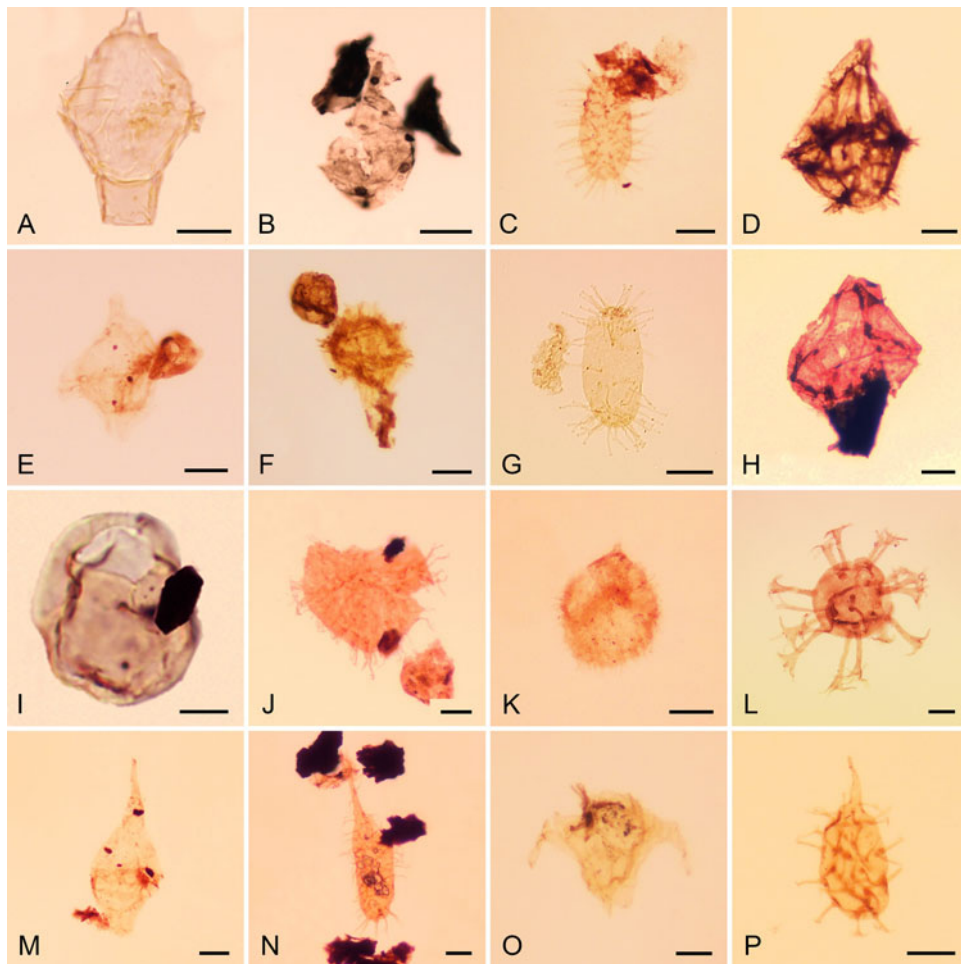
Figure 2. Selected palynomorphs from the Rollrock Section, Sverdrup Basin. Scale bar represents 20 μm. (a) *Tubotuberella rhombiformis* 384 m (V31). (b) *Pareodinia borealis* 132 m (U19-4). (c) *Tanyosphaeridium isocalamum* 408 m (T26). (d) *Gonyaulacysta adecta* 19.5 m (W29-3). (e) *Muderongia simplex* 505.5 m (V32-3). (f) *Nelchinopsis kostromiensis* 469.5 m (T37-4). (g) *Tanyosphaeridium magneticum* 406.5 m (U24-1). (h) *Rhynchodiniopsis cladophora* 19.5 m (V25-1). (i) *Chytroeisphaeridia chytroeides* 411 m (T30-3). (j) *Sentusidinium separatum* 361.5 m (V21-1). (k) *Trichodinium erinaceoides* 372 m (W33). (l) *Oligosphaeridium complex* 487.5 m (V26-2). (m) *Paragonyaulacysta capillosa* 195 m (D24-2). (n) *Gochteodinia villosa villosa* 487 m (U21-2). (o) *Muderongia tetracantha* 522 m (H23). (p) *Gochteodinia villosa* 402 m (T22).

analysis, which grouped similar samples together, providing the basis for palaeoenvironmental interpretations. The algorithm 'Ward's method' that joins clusters such that increase in within-group variance is minimised, was used. These analyses create dendrograms, clustering samples based on palynomorph content, joining similar pairs to a common node, with branch lengths indicating relative similarities (Paliy & Shankar 2016). Ward's method uses Euclidean distance, which assumes simplified linear relationships producing quick visuals of similarities between variables. Therefore, these clusters can be used to make broad interpretations about the samples and also provide a basis for further analytical statistical techniques.

The computer software program PAST was also utilised for detrended correspondence analysis (DCA). DCA is a multivariate statistical technique used to interpret species and sample ordination (Hill & Gauch 1980). DCA was created by Hill (1979) in order to compensate for the 'arch' and 'edge' effects inherent in other multivariate techniques such as principal component analysis (PCA). The arch (horseshoe) effect is the two-dimensional mathematical presentation of ecological data as a curve rather than a straight line, due to axis two in PCA being both uncorrelated with and dependent on axis one (Hill & Gauch 1980). To make accurate interpretations about these axes, they need to be uncorrelated and independent of one another. The edge effect is produced when compositional distances are not preserved. Two pairs of samples with the same

compositional distances will exhibit two different distances in the ordination, depending on where they are located on the first axis, resulting in compositional differences appearing greater in the middle of the gradient than at the ends (Hill & Gauch 1980). DCA overcomes the arch effect by dividing the first axis into segments, and then rescaling its axes, so the values on the second axis are equalised to a zero mean value. Rescaling ensures that equal compositional differences are represented by equal differences along the gradient, eliminating the edge effect (Hill & Gauch 1980).

The DCA was favoured herein over other multivariate techniques because floras, and their environment, usually have a non-monotonic and unimodal relationship rather than a linear one. DCA is also more suitable when dealing with zero data than PCA (Paliy & Shankar 2016). This becomes important when analysing long stratigraphic sections with frequent extinction and inception events controlled by time and environmental factors. DCA arranges data along two principal axes that represent variables such as environmental factors. The eigenvalues associated with each axis depict the extent to which each axis influences the data (Ramette 2007). Therefore, DCA can be utilised to observe and interpret species distribution and sample variation without the distortion seen in other multivariate techniques.

Correspondence analysis (CA) is an ordination method that can be used to display ecological information, which is inferred

from axes of eigenvalues representing directions of variation in a given assemblage data set. The eigenvalues derived are coefficients reflecting the degree of species dispersion along the axes (Ter Braak 1986; Kovach 1993).

Canonical correspondence analysis (CCA) is an extension of CA, in which an additional matrix, in this case of environmental data, is included in the analysis. Ordination axes (vectors) are added for known (environmental) variables (Ter Braak 1986; Kovach 1993). For example, this study uses elemental ratios derived from PXRF analysis.

Prior to undertaking statistical analyses, the data were processed to reduce statistical noise, resulting in more viable results. Firstly, samples with a count size of 25 or less (≤10% of highest count) were removed. This resulted in the removal of 13 samples. Secondly, taxa counts were converted into percentages to account for varying count sizes. Implementation of these techniques removed bias in the data towards taxa present in sparse and abundant samples. Consequently, these taxa are not overrepresented in any statistical analyses. Finally, taxa that had a cumulative count of less than 10% across the remaining samples were removed, preventing statistical anomalies, and decluttering the dataset. This resulted in the removal of 43 species. Without this data processing stage, the statistical noise and variability within the data set was too high to reveal meaningful patterns.

5. Results and discussion

5.1. Rollrock Section

5.1.1. Sample clusters.
In total, 200 samples were processed and analysed from the Rollrock Section. Recovery of marine palynomorphs varies within the formations, but the highest recovery comes from the lower Deer Bay Formation below the intra-Berriasian unconformity. Important dinoflagellate cysts are illustrated in Fig. 2. A detailed zonal scheme is presented in Ingrams et al. (2021).

Using the methodology outlined above, 187 samples and 93 taxa were analysed across the three formations of the Rollrock Section. Q-mode cluster analysis delineated three clusters and six sub-clusters (Fig. 3h), which correspond to the stratigraphic log of the Rollrock Section (Figs 3b, 2e). These clusters display strong stratigraphic control. The Ringnes Formation entirely comprises alternating local assemblage zones of clusters 1a and 1b. The Isachsen Formation contained one sample, placed into cluster 3a.

The Deer Bay Formation (250.5 m–522 m, Fig. 3c) contains all six sub-clusters but can be separated into three local assemblage zones (LAZs) based on distinct cluster assemblages (Fig. 3f). These LAZs occur as a result of shifts to new dinoflagellate cyst morphologies (Fig. 3f, g). Samples that delineate into the non-dominant cluster display reduced numbers of the dominant morphology. In Zone 1 the sample at 363 m delineating into cluster 2b coincides with a macrofossil horizon (Schneider et al. 2020), a transgressive surface, and the first occurrence of the chorate species Oligosphaeridium complex (Ingrams et al. 2021).

The base of LAZ 2 marks a horizon over which all data sets abruptly change, a common factor in other statistical analyses used on this interval. This is reflected in a dramatic increase of proximochorate cysts, from approximately 20% below this horizon, to approximately 50% above. Geochemical analysis also identifies this horizon, evidenced by sizeable increases in all detrital proxies analysed by PXRF (Appendix 2). Palynological evidence dates this horizon as Berriasian (Ingrams et al. 2021), the intra-Berriasian unconformity marking a hiatus within the Sverdrup Basin (Kemper 1975). The evidence presented here confirms that this unconformity occurs, and that it does not equate to the Jurassic–Cretaceous boundary.

5.1.2. Microplankton groups.
From DCA of the dinoflagellate cyst taxa found within the Rollrock Section (Fig. 4) five distinct groups were identified. These DCA groups each reflect closely associated taxa whose distribution was controlled by similar environmental factors. These groups are correlative with stratigraphic distributions of the previously delineated clusters (Fig. 5; for a results summary see Table 1). Higher values along axis 1 commonly correlate to taxa found more abundantly in younger samples, indicating a strong stratigraphical control over the data set.

The scale on axis 1 represents the standard deviation (SD) of taxon turnover. A taxon is expected to appear, rise to its mode, and disappear within four SD units (Hill & Gauch 1980). This implies that taxa which are more than four SD units apart on axis 1 should have no overlap. Generally, a change of approximately 50% in sample assemblage composition should occur within one SD unit (Hill & Gauch 1980).

Data from the DCA plot of the Rollrock Section are affected by variables represented by the first two axes, which possess eigenvalues of 0.37 (axis 1) and 0.15 (axis 2). Chorate taxa plot with high values on axis 1, while proximochorate taxa plot with high values on axis 1 and low values on axis 2. Gonyaulacysta species plot with low axis 1 values. Therefore, it is possible that axis 1 represents nutrient availability or turbidity.

5.1.3. Palaeoenvironmental analysis.
In order to determine what the palynological and statistical trends are reflecting, a link needs to be established to a controlling environmental factor. CCA of palynological and elemental data has previously been used to delineate controlling environmental factors (e.g., Hammer & Harper, 2006). In this study, this method has been applied to the taxonomic groups previously identified by cluster and DCA analysis (Fig. 6). A positive relationship between the aluminium/silica (Al/Si) ratio and cluster 3 was observed, and a negative relationship with clusters 1 and 2a (Figs 3h, 6). The rubidium/strontium (Rb/Sr) ratio shows a weak positive relationship with cluster 2b. The zirconium/rubidium (Zr/Rb) ratio displays an inverse trend to that of Al/Si, with a negative relationship with cluster 3 and a positive relationship with clusters 1 and 2a.

The Rb/Sr is a strong proxy for weathering and coastline proximity. When this ratio is high, the sediment is identifiably more immature. Rubidium is a highly leachable element; thus, its presence in increased amounts indicates that the source sediment is originating from an area exposed to a high degree of weathering leading to higher nutrient levels within the sediment load. Zr/Rb is an indicator of low nutrient levels, and therefore, indicates the opposite to Rb/Sr. Zr/Rb is also used to track changes in sediment grain size (Calvert & Pedersen, 2007), as Zr often resides in coarser grained particles than Rb. Al/Si is a reliable indicator of clay content in the sediment. High Al/Si values are associated with lower energy, deeper water environments, where Al is an indicator of the clay component of the sediment load and Si is an indicator of coarser grained material. Because all samples were taken from roughly similar fine-grained lithology, it is inferred herein that samples with lower values of this ratio are siltier than those with a higher ratio.

While CCA is strongly influenced by stratigraphy, some conclusions can still be drawn. There is a clear divide between samples from above and below the aforementioned intra-Berriasian unconformity (Fig. 6). Sediments generally control nutrient availability, and those deposited above the unconformity are much more clay rich, and as such indicate a lower energy, more nutrient depleted environment.

5.2. Post intra-Berriasian unconformity

5.2.1. Sample clusters.
In order to remove the stratigraphic controls present in the data, the Deer Bay Formation above the
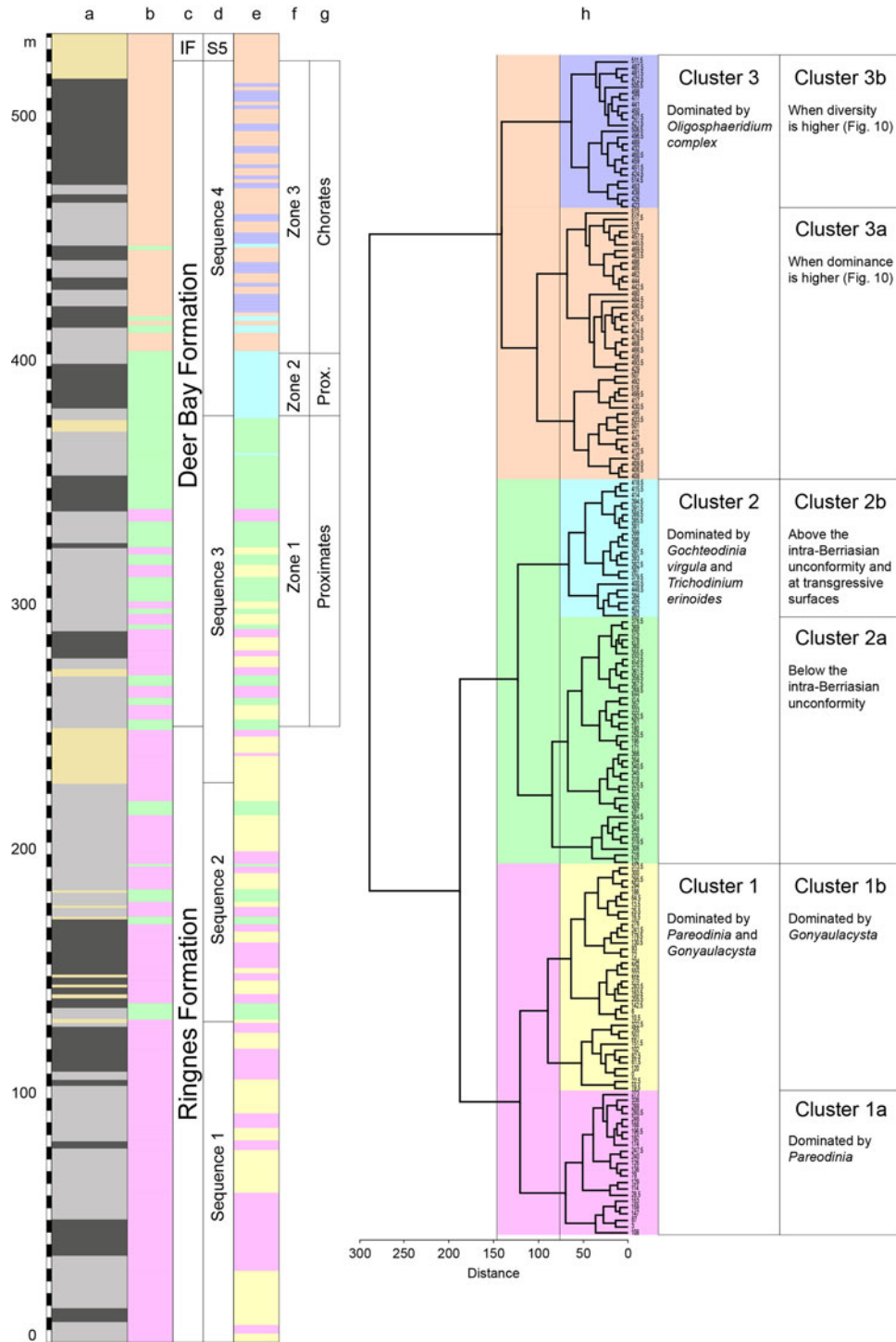
Figure 3. Statistical data generated by marine palynomorphs of the Rollrock Section. (a) Lithology. (b) Cluster association. (c) Formations. (d) Sequences. (e) Sub-cluster association. (f) Local assemblage zones. (g) Dominant process type. (h) Q mode cluster dendrogram.

unconformity has been examined separately, with samples taken systematically every 1.5 m. Using the methodology outlined in the previous sections, the upper Deer Bay Formation and a singular sample from the Isachsen Formation were analysed using Q-mode cluster analysis resulting in four clusters being delineated (Fig. 7d).

When comparing these clusters to the lithostratigraphy of the Rollrock Section four clear zones are observed (Fig. 7c). Cluster uDB3, delineated from the upper Deer Bay Formation, is directly linked to cluster 2b from the whole section analysis. Consequently, this cluster/sub-cluster is confirmed to be controlled by an external environmental factor rather than by chronological changes. Clusters uDB1, uDB2 and uDB4 (Fig. 7d) are

correlated to cluster 3 from the whole section analysis (Fig. 3h), adding further emphasis to the strong stratigraphical control of the whole section. On the other hand, this result confirms that clusters delineated during separate analysis of the upper Deer Bay Formation are controlled by non-chronological factors.

5.2.2. Microplankton groups. The taxa present in the upper Deer Bay Formation were subjected to a separate DCA (Fig. 8). Using the methodology detailed above, a further 23 taxa were discarded, resulting in 69 taxa being analysed across the 88 viable samples of the upper Deer Bay Formation. The eigenvalues of axis 1 and axis 2 (0.25 and 0.13, respectively) show a positive correlation between samples and taxa. Cumulative percentages
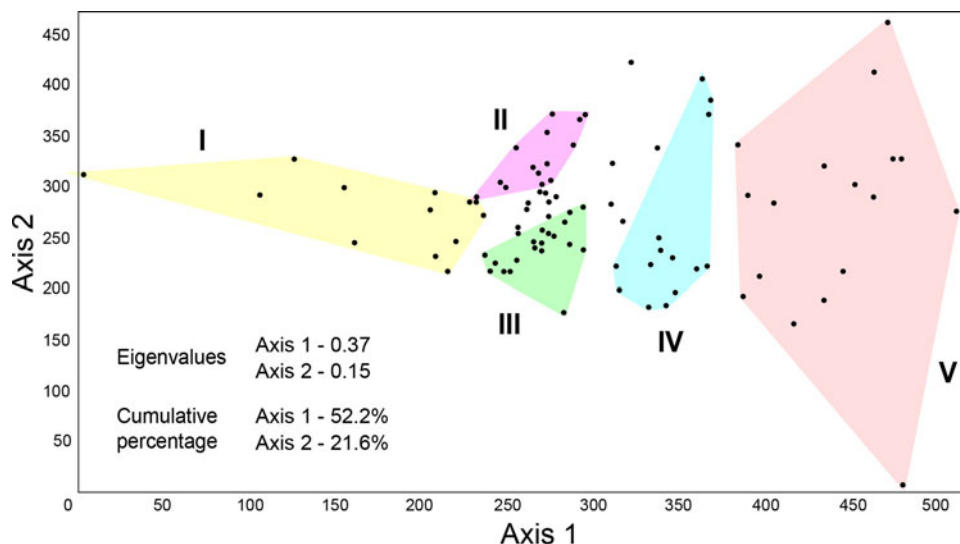
Figure 4. Detrended correspondence analysis bi-plot output showing taxa ordinated in a two-dimensional plane. Convex hulls embrace associated groups of taxa. Taxa outside the hulls are not associated with any of the groups.

show that axis 1 accounts for twice the amount of variance of axis 2. While the eigenvalues might appear low, count data, even after filtering, is inherently noisy, and these values are typical when dealing with palynomorph data sets that have a high number of variables (Daly *et al.* 2011).

From DCA of this part of the section it is possible to identify four groups of taxa and four outlying taxa (Fig. 8). The four groups vary in distribution and abundance (Table 2; Fig. 9). Plotting the distributions of these groups highlights trends that are not apparent from analysis of the entire section.

Group uDBIV contains many poorly preserved proximate taxa that do not directly correspond to the delineated clusters. The taxa in this group, such as *Pareodinia borealis* and *Pareodinia ceratophora* are present in the majority of samples, and as such can be considered to be the dominant autotrophic population of the section. These taxa remain largely unaffected by

environmental controls exerted on the section. A similar pattern is observable in group uDBII.

The taxa grouped within uDBIII (Table 2) are episodically common in this part of the section (Fig. 9). Where uDBIII becomes the most abundant group, samples delineate into cluster uDB3. Where uDBIII is not the most abundant group and numbers of taxa found within group uDBII are low (Table 2), samples delineate into cluster uDB4 (Fig. 9). In the whole section analysis, the uDBII pattern is overprinted by the presence of chorate species of the genus *Oligosphaeridium*, which are almost entirely absent in the section below the unconformity.

5.2.3. Palaeoenvironmental analysis. To reveal links between sample clusters, DCA taxa groups and environmental factors, CCA was undertaken using PXRF element ratios as environmental proxies. Three types of positive relationships were recovered (Fig. 10).
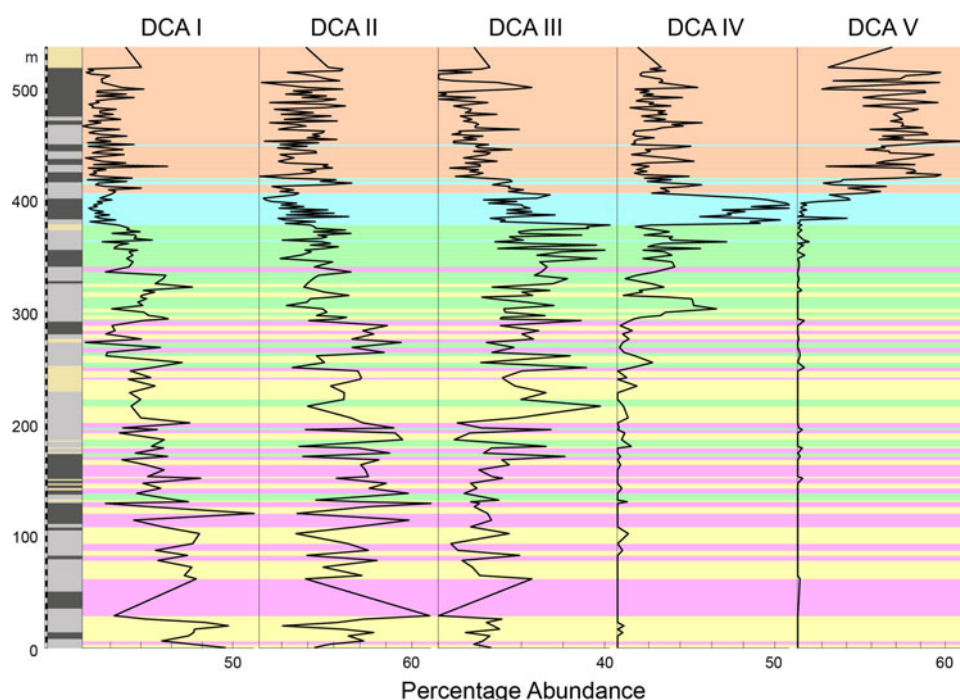

Figure 5. Stratigraphical distribution of the five detrended correspondence analysis groups identified in Figure 4. Coloured bands represent sample Q-mode clusters identified in Figure 3i and listed in Appendix 2.

Table 1. Summary of stratigraphical and statistically important taxa influencing detrended correspondence analysis groups linked to cluster association and stratigraphical occurrence.

Group (Fig. 4)	Significant taxa	Cluster association (Fig. 3i)	Stratigraphical occurrence (Fig. 5)
I	*Gonyaulacysta adecta, Gonyaulacysta jurassica*	1b	More dominant at base of the section (Ringnes Formation).
II	*Pareodinia cretophora, Pareodinia borealis, Pareodinia* spB, *Cribroperidinium* spp, *Atopindinium prosatum, Dingodinium minitum,*	1a	More dominant at base of the section (Ringnes Formation) and at the base of the Deer Bay Formation.
III	*Biorbifera johnewingii, Sentusidinium fillatum, Tubotuberella rhombiformis, Tubotuberella apatela*	2a	216 m–264 m and 288 m–379.5 m.
IV	*Tanyosphaeridium isocalamum, Impletosphaeridium ehrenbergii, Gochteodinia virgula, Gochteodinia judilentinae, Sentusidinium separatum, Trichodinium erinaceoides*	2b	Very low values until 250 m where a series of spikes can be observed. The first and smallest spike is at 268.5 m, the second spike occurs between 303 m–312 m, the third at 363 m. The largest increase in this group occurs immediately after the unconformity present at 379.5 m until 406.5 m.
V	*Oligosphaeridium complex, Oligosphaeridium asterigerum, Oligosphaeridium albertense, Oligosphaeridium porosum, Odontochitina operculata*	3	Spikes at 363 m and 400 m. Dominant after 405.5 m.

A close association of uDB1 and uDB2 is observed (Fig. 10) as their palynofloral composition is similar (Fig. 7d). uDB2 has a slightly stronger positive relationship with Al/Si indicating deposition in more clay rich conditions. Because all the samples are taken from roughly the same lithology and Zr/Rb, as a proxy of grain size, has only a weak relationship with uDB4, it is clear that another factor must also be controlling distribution. However, the uDB4 group contains many samples where preservation is of a significantly lower standard. Likewise, many of the palynomorphs found in these groups are degraded and are only identifiable to genus level. Therefore, it is possible that the change in grain size has affected preservation, causing degradation of palynomorphs either during or after deposition.
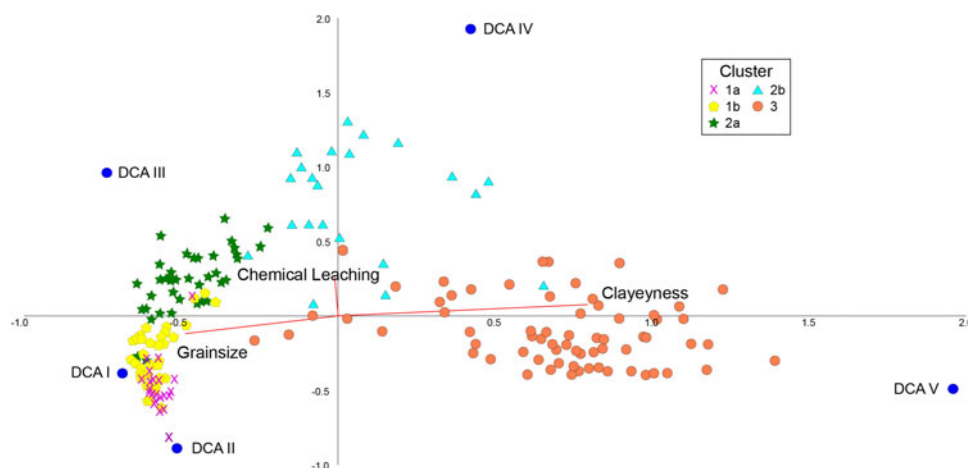
5.3. Sequence stratigraphic analysis

5.3.1. Third order sequences. The Rollrock Section is contained within the mid Permian–Hauterivian first order sequence and the Oxfordian–Hauterivian second order sequence *sensu* Embry (1993) and Embry *et al.* (2019). The multidisciplinary approach outlined above, combining sedimentology, palynology and geochemistry, has revealed five third order sequence stratigraphic cycles in the mudstone-dominated Rollrock Section (Fig. 11), which are compared to the sequences identified by Embry (1993) and Embry *et al.* (2019) (Table 3).

Two key sequence stratigraphic surfaces, that is, sequence boundaries (SBs) and maximum flooding surfaces (MFSs), can generally be identified using marine palynology. Generally, SBs are represented by a relative loss in dinoflagellate cyst abundance and diversity. In contrast, MFSs are represented by the highest relative abundance and diversity of dinoflagellate cysts, resulting from the expansion of habitats associated with transgressions and a reduction in relative energy levels, allowing for a more complete plankton (Morley, 1996). The Rollrock Section displays varying dinoflagellate cyst abundance patterns, which are used herein as the main palynological indicator for identifying sequences.

In a shelf environment, cyst bearing dinoflagellates bloom with greater diversity in relatively deep and less turbulent waters (e.g., Posamentier *et al.* 1988; Wornardt, 1993; Armentrout, 1996; Morley, 1996). In contrast, assemblages in turbulent or stressed environments are often dominated by a few species (e.g., Armentrout, 1996). Utilising a combination of dinoflagellate cyst diversity and sedimentology, a sequence stratigraphic framework has been defined for the Rollrock Section, comprising three complete and two incomplete sequences (Table 3).

Sequence 1 (0 m–141 m): Sequence 1 is characterised by sparse data and dinoflagellate cysts are often highly degraded, resulting from both depositional and diagenetic processes. Sequence 1

Figure 6. Canonical correspondence analysis displaying environmental controls over sample cluster association and detrended correspondence analysis taxa groupings.
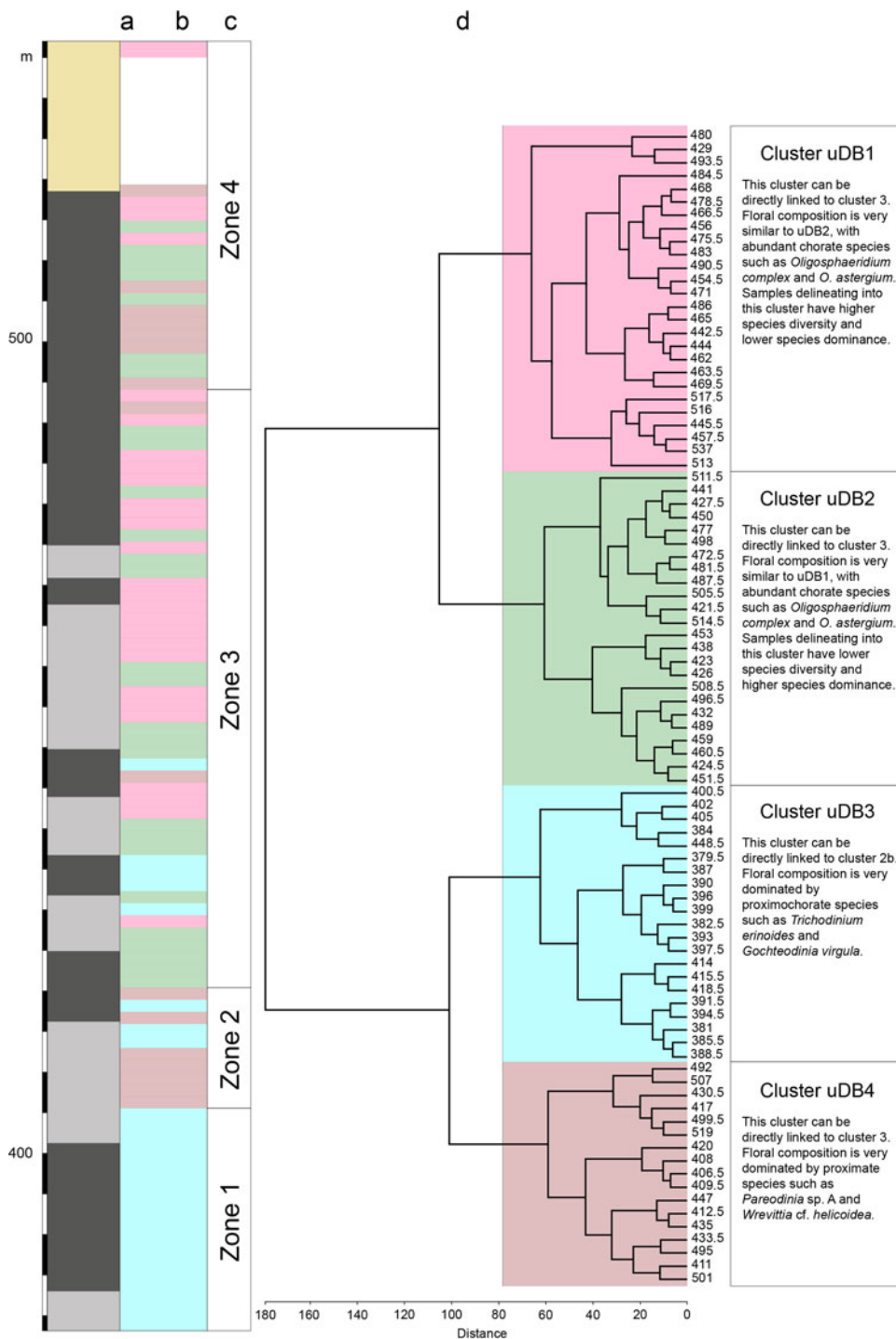
Figure 7. (a) Lithology. (b) Cluster association. (c) Zones. (d) Cluster dendrogram of the upper Deer Bay Formation.

covers the lower portion of the logged Ringnes Formation. The top of sequence 1 is defined by a 2 m thick fine grained sandstone unit at 141 m (Schneider *et al.* 2020). Within sequence 1, dinoflagellate cyst diversity is very low from 22.5 m–61.5 m, but this is partially caused by poor preservation and recovery. An approximate 20 m cyclicity in dinoflagellate cyst diversity is observable between 61.5 m and the SB. Whether this represents fourth order cyclicity is undetermined. The base of sequence 1 lies within the Oxfordian, with the first identifiable Kimmeridgian level at 132 m (Ingrams *et al.* 2021). With regard to age, this sequence correlates with sequence 8 of Embry (1993) and with the bottom half of the base Oxfordian sequence of Embry *et al.* (2019) (Table 3). All samples taken from this sequence plot entirely within cluster 1 (Fig. 3b).

Sequence 2 (141 m–230 m): Sequence 2 is composed of mudstones of the upper Ringnes Formation. The upper SB is defined as the base of the first very fine-grained sandstone unit with large concretions (230 m, Fig. 3), which marks the upper part of the Ringnes Formation (Schneider *et al.* 2020). Dinoflagellate cyst diversity changes cyclically within an overall increasing trend to 196.5 m. This level contains the highest dinoflagellate cyst diversity, corresponds to the second of three macrofossil horizons containing *Buchia rugosa* (Schneider *et al.* 2020), and is identified as the MFS (Fig. 11). The cycles below the MFS are on average 15 m thick and relatively consistent and could be argued to represent fourth order sequence cycles. However, due to the lack of more detailed evidence, they are not identified as such within this study. Above the MFS, dinoflagellate cyst diversity
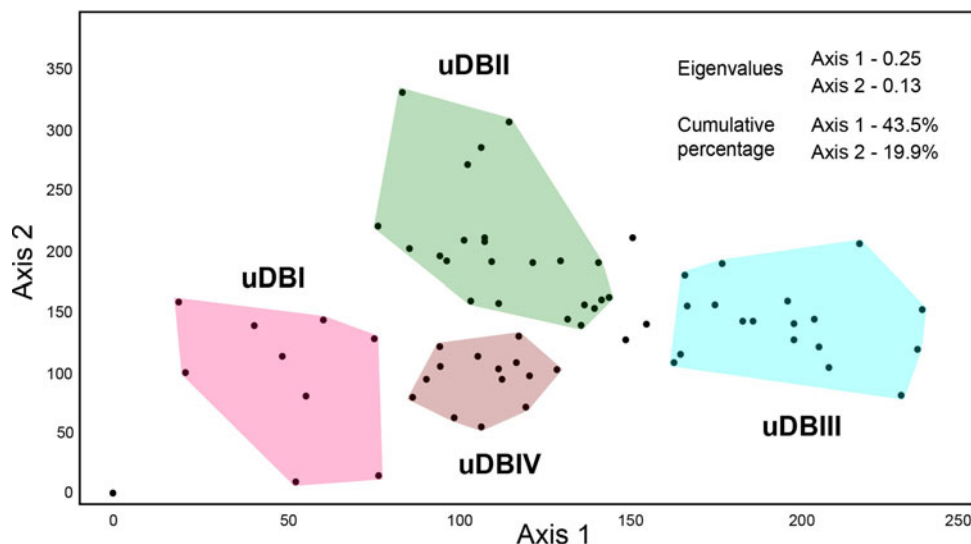
Figure 8. Detrended correspondence analysis bi-plot of taxa recovered from the upper Deer Bay Formation. Shaded areas indicate close taxa association.

trends cyclically downwards towards the SB. The youngest diversity peak occurs 9.5 m above the MFS and 14 m below the SB. Ingrams *et al*. (2021) determined the age of this sequence as middle Kimmeridgian–late Tithonian. Schneider *et al*. (2020) assigned the *B. rugosa* horizons at 192, 196.5, and 196.8 m to the early Tithonian *B. rugosa* zone. This sequence correlates with sequence 9 of Embry (1993) and the upper half of the base Oxfordian sequence of Embry *et al*. (2019) (Table 3). The MFS of this sequenced was hypothesised by Embry (1993) to be close to the Kimmeridgian–Tithonian boundary based on evidence from *Buchia* bivalves reported by Balkwill (1983). The samples taken from this sequence mostly delineate into cluster 1, with four samples delineating into cluster 2 (Fig. 3h).

Sequence 3 (230 m–379.5 m): Sequence 3 comprises siltstones and very-fine grained sandstones from the upper Ringnes Formation and the lower mudstones of the Deer Bay Formation. The SB is located at 379.5 m at a thin, well indurated siltstone bed (Schneider *et al*. 2020), which corresponds with the intra-Berriasian unconformity. Dinoflagellate cyst diversity increases cyclically up to 292.5 m and decreases cyclically above until the SB (Fig. 11). These cycles are on average 12.5 m thick (10.5 m–17.5 m), potentially reflecting fourth order sequences. Sequence 3 was dated as Tithonian–Berriasian by Ingrams *et al*. (2021). Several macrofossil horizons occur within the regressive systems tract of this sequence, containing ammonites and *Buchia* bivalves described in detail in Schneider *et al*. (2020), which confirm the Tithonian–Berriasian age. This sequence correlates with sequence 10 of Embry (1993) and the base Tithonian sequence of Embry *et al*. (2019) (Table 3).

Recent finds of *Borealites fedorovi*, *Buchia okensis* and *O. complex* indicate an (early) Berriasian age below the sequence boundary at the unconformity, correlating with the age proposed by Embry *et al*. (2019). The MFS for the sequence described by Embry (1993) occurs close to the base of the sequence, creating a large regressive systems tract. The MFS in the present study is also seen to be near the base of the sequence creating a large highstand systems tract. The samples in this sequence mostly delineate into cluster 1 below the MFS and into cluster 2 above, although there are exceptions in both parts of the sequence (Fig. 3b). The samples collected from the lowstand systems tract (230 m–251 m) all delineate into cluster 1 (Fig. 3b).

Sequence 4 (379.5 m–524.5 m): Sequence 4 comprises mudstones in the upper Deer Bay Formation. The SB is located at the base of the Isachsen Formation (524.5 m). Like in the

preceding two sequences, dinoflagellate cyst diversity trends cyclically upwards until it reaches the MFS (411 m), before cyclically trending downwards towards the SB (Fig. 11). Sequence 4 was dated as late Berriasian–Valanginian based on palynology (Ingrams *et al*. 2021) and as broadly Valanginian based on sparse macrofauna (Schneider *et al*. 2020). This sequence roughly correlates with an unnamed third order sequence of Embry (1993) that incorporates the Berriasian and terminates at the top of the Awingak Formation. However, the Awingak Formation does not occur in the more distal Rollrock Section. The samples from this sequence delineate into cluster 2b below 405 m and mostly into cluster 3 above. Unlike for previous sequences, there is a greater degree of variation in dinoflagellate cyst diversity in this sequence, and a more detailed analysis was undertaken (Fig. 12).

Embry (1993) hypothesised that the Upper Jurassic to Lower Cretaceous sedimentary succession of the Sverdrup Basin can be assigned to six third order sequence stratigraphic cycles. The oldest three cycles range from the Oxfordian to the early Kimmeridgian, the late Kimmeridgian to the early Tithonian, and the late Tithonian to the Jurassic–Cretaceous boundary. The three Cretaceous sequences were not dated. However, the upper boundary of the sixth third order sequence is the sub-Hauterivian unconformity, positioned within the Isachsen Formation, but stratigraphically above the succession studied herein (see also Galloway *et al*. 2015). This concept was updated by Embry (2011), Embry & Beauchamp (2019) and Embry *et al*. (2019) who divided the Upper Jurassic to lowermost Cretaceous succession into three third order cycles: base Oxfordian to base Tithonian; base Tithonian to mid-Berriasian/Valanginian; and mid-Berriasian/Valanginian to Hauterivian. The poorly resolved boundary age of the second and third cycles indicates that this level was taken at the intra-Berriasian unconformity.

The discrepancy in the number of third order sequences can be attributed to the methodology used to identify sequences. Embry *et al*. (2019) used transgressive–regressive (T-R) sequences to determine boundaries, where the maximum regression surface (MRS) is taken as the sequence boundary. This enables the discovery of tectonically generated, large magnitude SBs with associated unconformities. The present study utilises a different sequence stratigraphic terminology, where a sequence is defined by correlative conformities (e.g., Van Wagoner, 1988; Nichols, 2009), expressed in the Rollrock Section as sandstone bodies. The difference between the two approaches becomes most

Table 2 Summary of linkage of detrended correspondence analysis groups from the upper Deer Bay Formation with cluster analysis and stratigraphical occurrence.
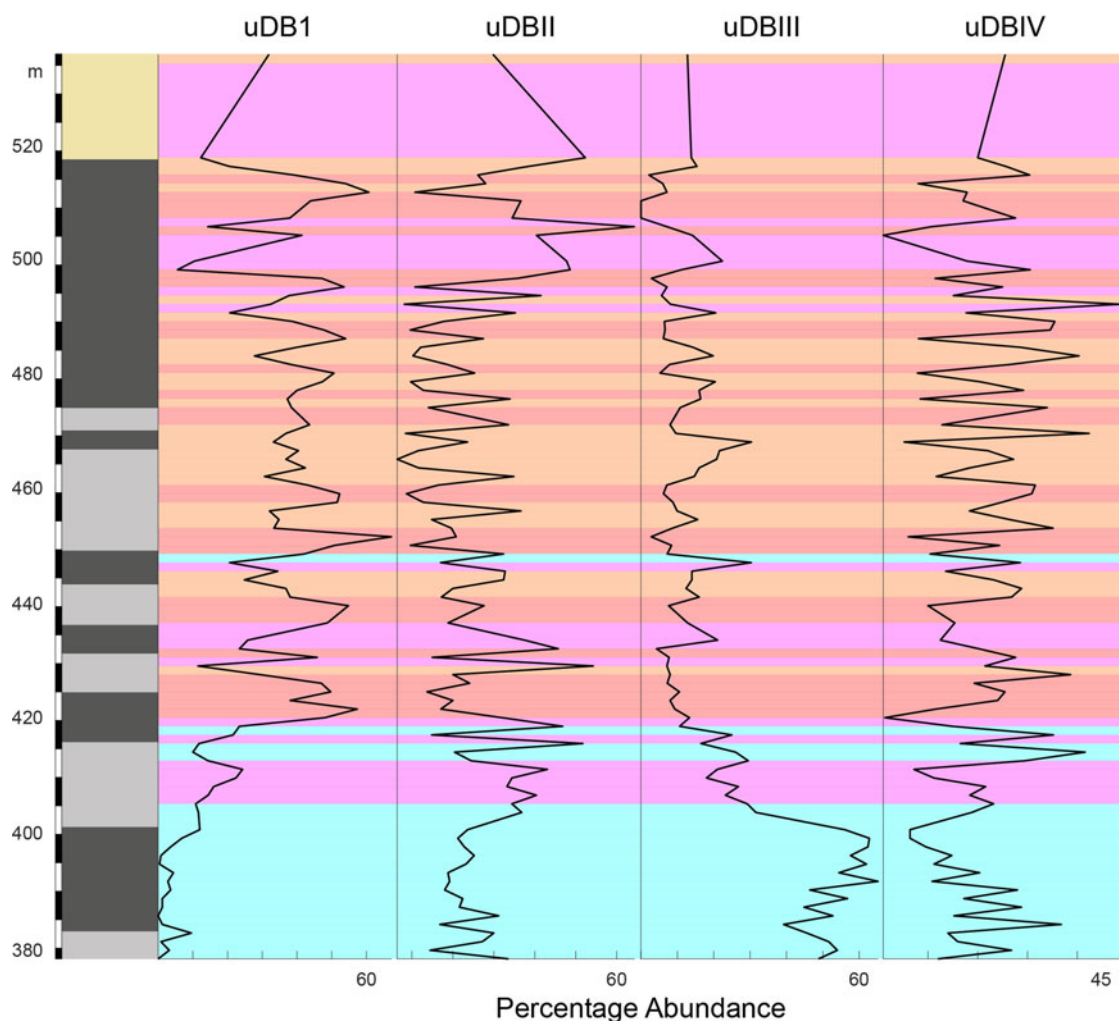
Group (Fig. 8)	Significant taxa	Cluster association (Fig. 7d)	Stratigraphical occurrence (Fig. 9)
uDBI	*Oligosphaeridium complex, Oligosphaeridium asterigerum, Gochteodinia villosa villosa*	uDB1, uDB2	Upper section of the upper Deer Bay Formation.
uDBII	*Muderongia simplex, Pareodinia* sp. A, *Odontochitina operculata*	uDB4	Present in whole of the upper Deer Bay Formation in stable numbers.
uDBIII	*Trichodinium erinoides, Gochteodinia virgula, Lanterna* sp. A	uDB3	379.5 m–400 m.
uDBIV	*Pareodinia borealis, Pareodinia cretophora*	none	Present in the majority of samples.

obvious when comparing the top of the sequence that begins at the post-Berriasian unconformity. Embry *et al.* (2019) place the top of this sequence at the sub-Hauterivian MRS. Herein, the upper boundary is placed at the inception of the Isachsen Formation, and the Valanginian part of the Isachsen Formation conforms to an additional third order sequence.

Embry *et al.* (2019) identified a third order sequence from the base Oxfordian to the base Tithonian (Table 3). Both this study and Embry (1993) split this sequence into two different sequences (Table 3). The boundary between these two sequences does not meet the criteria of a large-magnitude boundary generated by tectonically driven base level changes rather than by eustasy (Embry *et al.* 2019). Therefore, the sequence boundary between sequences 1 and 2 in the Rollrock Section is controlled by eustacy rather than tectonic activity.

5.3.2. Fourth order sequences, upper Deer Bay Formation. Applying the methodology outlined above, dinoflagellate cyst diversity and sedimentology have been used to determine ten fourth order sequences (Table 4). Fourth order low stand systems tracts are unidentifiable since the upper Deer Bay Formation is entirely composed of mudstone and siltstone. Consequently, the data were studied as a T-R system. Sequence boundaries and transgressive surfaces were identified by changes in the diversity curve, the former being identified by minimum diversity and the latter by maximum diversity (Morley, 1996).

By comparing these fourth order sequences with the distribution of taxa within DCA groups uDBI–uDBIV several patterns are observable (Fig. 12). There is a clear separation of taxa occurring in transgressive and regressive periods.

Figure 9. Stratigraphical distribution of the detrended correspondence analysis groups identified in Figure 8. Coloured areas indicate sample cluster association derived from Figure 7d.
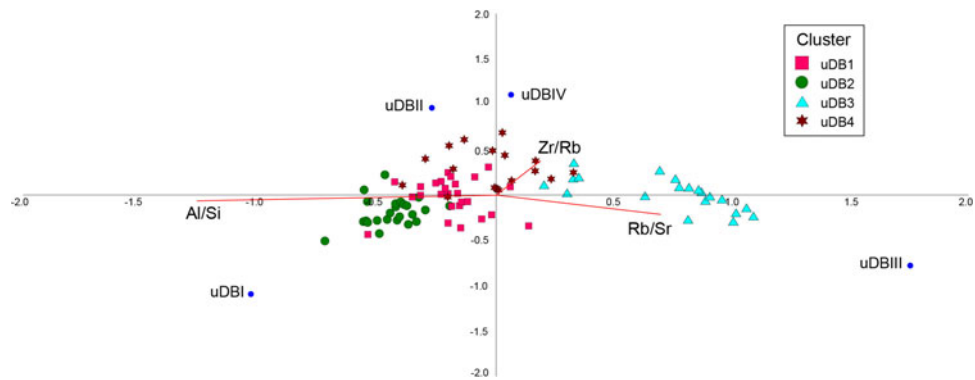
Figure 10. Canonical correspondence analysis displaying environmental controls over sample cluster association and detrended correspondence analysis taxa groupings taken from the upper Deer Bay Formation.
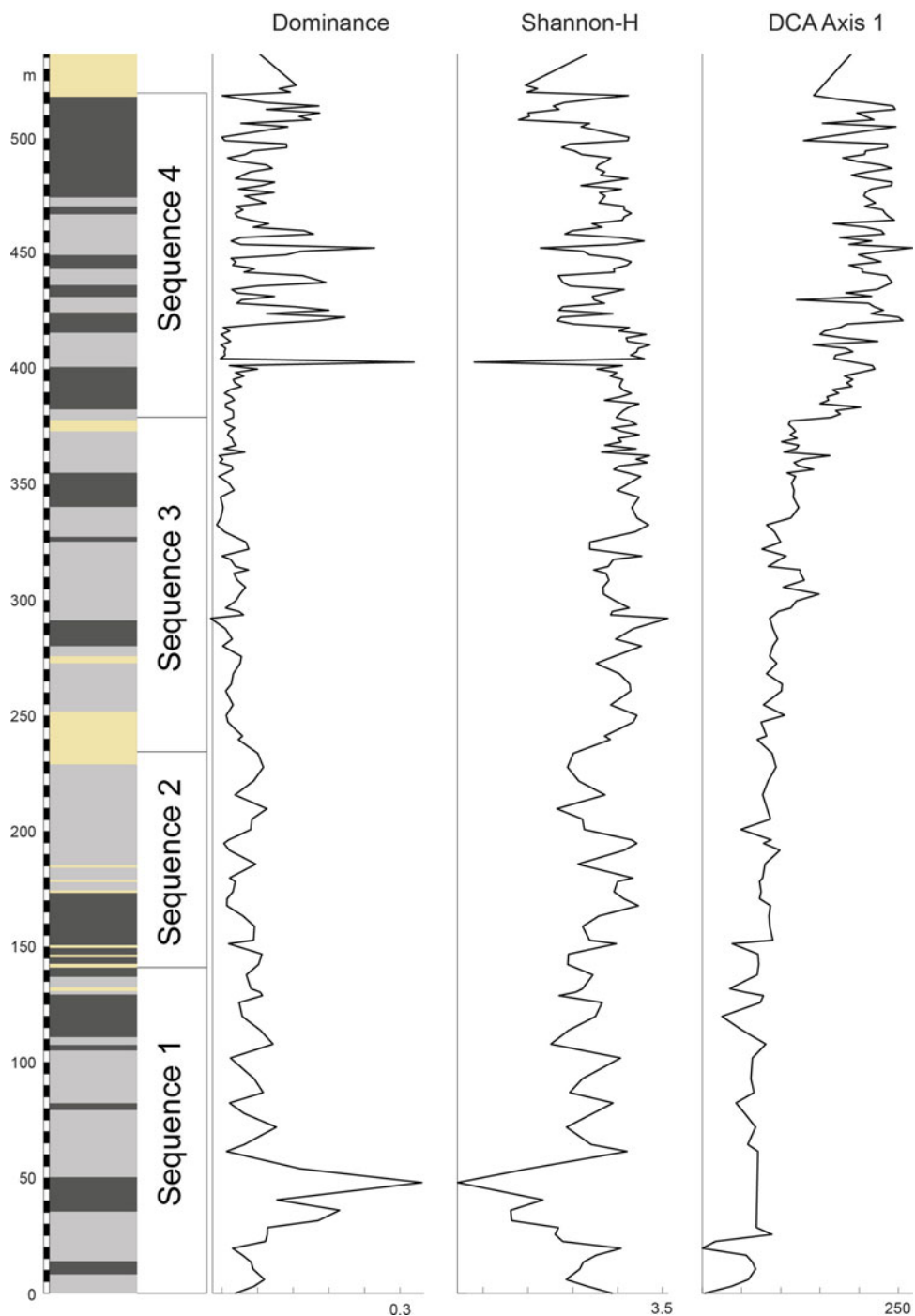

Figure 11. Stratigraphic distribution of values of dominance, Shannon-H diversity and detrended correspondence analysis Axis 1, calculated for marine palynomorphs.

Table 3 Third order sequence stratigraphic packages identified in this study with an age comparison to those identified by Embry (1993) and Embry *et al.* (2019).

Sequence	Rollrock Section height	Age	Authority	(Embry 1993: Age)	(Embry *et al.* 2019: Age)
1	0 m–141 m	Oxfordian–Kimmeridgian	Palynology (Ingrams *et al.* 2021)	Oxfordian- early Kimmeridgian	Oxfordian–Tithonian
2	141 m–230 m	Kimmeridgian – Tithonian	Palynology (Ingrams *et al.* 2021) Macropalaeontology (Schneider *et al.* 2020)	late Kimmeridgian –early Tithonian	
3	230 m–379.5 m	Tithonian–Berriasian	Palynology (Ingrams *et al.* 2021) Macropalaeontology (Schneider *et al.* 2020)	late Tithonian–Jusassic Cretaceous boundary	Tithonian– mid-Berriasian
4	379.5 m–524.5 m	Late Berriasian – Valanginian	Palynology (Ingrams *et al.* 2021) Macropalaeontology (Schneider *et al.* 2020)	Berriasian?	Mid- Berriasian–Hauterivian
5	524.5 m+	Valanginian – ?	Palynology (Ingrams *et al.* 2021)	?	

The DCA group IV/uDBIII dominates the section from the third order SB up to 405 m. While the group is present throughout sequence 4, it cyclically declines (Fig. 12), being most abundant in the third order transgressive systems tract immediately above the unconformity. Moreover, this group is seen to increase in abundance above transgressive surfaces, during regressive periods. Group uDBIII is composed primarily of proximochorate cysts (e.g., *Trichodinium erinaceoides* and *Gochteodinia virgula*), which display a strong positive relationship to uDB3 (Fig. 7d) and fourth order highstand systems tracts (Fig. 12), Rb/Sr (Fig. 10). The break in sedimentation, associated with the unconformity, and the increase of proximochorate species making up uDBIII, suggest that these taxa outcompete other species during periods of lower relative sea level.

Similarly, the abundance of group uDBII increases above transgressive surfaces. However, uDBII displays reduced abundances near the bottom of the sequence, where the respective taxa were outcompeted by those in uDBIII (Fig. 12). In contrast, group uDBII displays an increase in abundance towards the top

of sequence 4, because the final two fourth order sequences were generally shallower than those that preceded them. Within this interval, nutrient flux was different from that in the basal part of sequence 4, and no group uDBIII was established (Fig. 10).

While group uDBIV has the same stratigraphical pattern as group uDBII, a different conclusion can be drawn. uDBIV displays generally higher abundances of taxa than uDBII and contains taxa that are present in relatively stable numbers throughout the upper Deer Bay Formation. This suggests that they maintained stable populations, while, at the same time, variations in the abundance of the other groups provide evidence of changes in palaeoecology.

Group uDBI occurred in higher frequencies below transgressive surfaces, during transgressive periods, but is poorly represented in the first two fourth order sequences. This pattern suggests that species in this group outcompeted other taxa during periods of relatively high sea level. There are some anomalies, for example, at 430.5 m, where the abundance of group uDBI decreased within a transgressive systems tract. However, in the
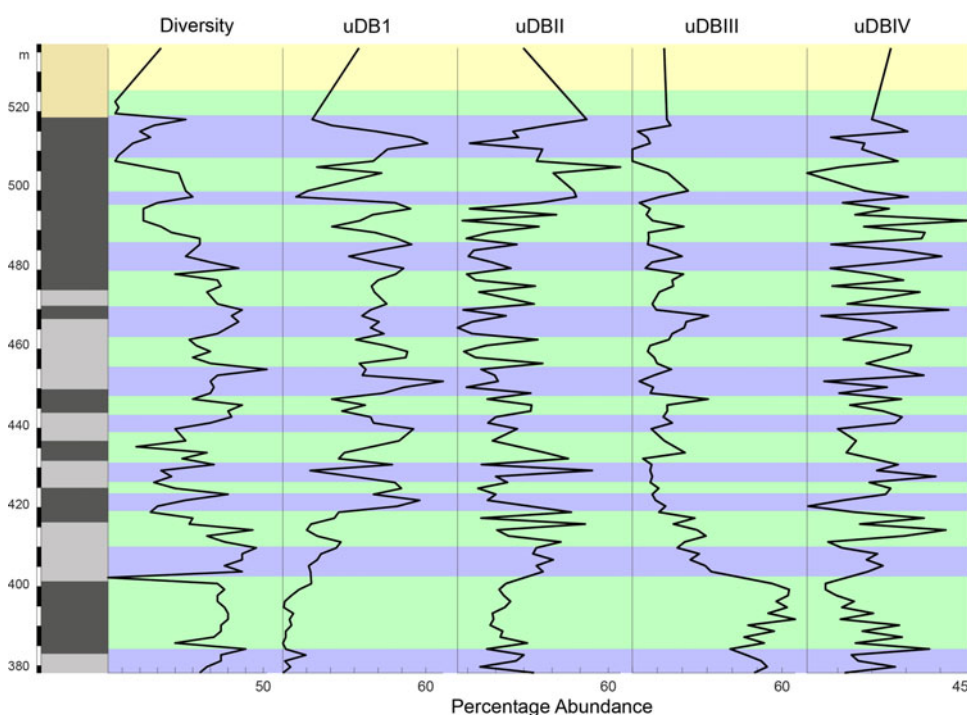

Figure 12. Stratigraphic distribution of detrended correspondence analysis taxa groups of the upper Deer Bay Formation identified in Figure 8. Green bands represent fourth order regressive systems tracts, blue bands represent fourth order transgressive systems tracts, the yellow band represents a third order lowstand systems tract.

Table 4 Intervals, thicknesses and transgressive surfaces of fourth order sequence stratigraphic cycles identified in the upper Deer Bay Formation.

Fourth order sequence	Rollrock Section height	Thickness	Transgressive surface
1	379.5 m–403.5 m	14 m	385.5 m
2	403.5 m–420 m	16.5 m	411 m
3	420 m–427.5 m	7.5 m	424.5 m
4	427.5 m–439.5 m	12 m	432 m
5	439.5 m–448.5 m	9 m	444 m
6	448.5 m–463.5 m	15 m	456 m
7	463.5 m–480 m	16.5 m	469.5 m–471 m
8	480 m–496.5 m	16.5 m	487.5 m
9	496.5 m–507 m	10.5 m	499.5 m −501 m
10	507 m–521 m	14 m	518 m?

latter sample this decrease is primarily down to poor preservation rather than ecological control. Group uDBI, composed primarily of chorate cysts such as *O. complex*, displays strong positive relationships to fourth order transgressive tracts (Fig. 12), Al/Si values (Fig. 10) and to uDB1 and uDB2 (Fig. 7d).

From these data, DCA axis 1 (Fig. 8) is interpreted to reflect nutrient availability and/or water depth. The proximochorate dominated uDBIII group is a proxy for more proximal, high energy, nutrient rich conditions, while the chorate dominated uDBI group is a proxy for distal, low energy, reduced nutrient conditions. These two groups show a departure from normal conditions, represented by groups uDBII and uDBIV, and as such are only proxies relative to the original state. Group uDBI is interpreted to reflect deeper and calmer water masses. Group uDBIII in contrast reflects shallower and more turbid environments.

5.4. Microplankton paleobiology

Dinoflagellates, like all other organisms, have evolved to meet the conditions of specific habitats. The evidence presented here shows two main morphological adaptations that benefit organisms in specific environments. Taxa possessing chorate processes are observed to dominate relatively deeper calmer, conditions, while taxa possessing proximochorate processes are observed to dominate relatively shallower, more turbid conditions.

Long processes on chorate cysts are associated with deeper-water, lower-energy, warmer conditions (e.g., Poulsen & Riding, 2003; Carvalho *et al.* 2016). Processes have been hypothesised to be floatation devices that are a necessary adaptation in warmer waters (Lentin & Williams 1980), because the specific gravity of water falls at higher temperatures (Poulsen & Riding 2003), as molecules gain more energy and expand. In modern samples, process length has been directly correlated to salinity and sea surface temperatures (e.g., Mertens *et al.* 2009, 2012a, 2012b). While it is possible that this method could be applied to different genera in the Mesozoic, analysis of the data collected from the Rollrock Section indicate it cannot be directly applied to this study. The palynomorphs recovered from the Rollrock Section have been diagenetically altered and as such display high amounts of intraspecific variation. For example, processes of *O. complex* were measured from two samples (456.0 m and 463.5 m; a fourth order transgressive surface and sequence boundary, respectively) from specimens with low amount of visible alteration. However, no meaningful data were recovered, with process lengths ranging from 19 μm to 33 μm. Variation within a single specimen can range between 3 μm and 9 μm, and no discernible difference in average process length between the two samples was observed.

Oligotrophic, warmer, and deeper habitats in modern oceans are observed to be dominated by nutrient stress tolerant taxa (Smayda & Reynolds 2003). These are typically very large, slow growing and often highly ornamented species (Smayda & Reynolds 2003). In this study, species of *Oligosphaeridium* are interpreted to have dominated assemblages in similar habitats.

In previous studies of dinoflagellate cysts from the Sverdrup Basin, frequency increases in small spinose cysts during several intervals throughout the Jurassic and Cretaceous were identified (Pocock 1976; Ingrams *et al.* 2021). These cysts were never formally identified by Pocock (1976), but instead were described as ovoid with definite polarity. This lead Davies (1983) to hypothesise that these cysts either represented *Exochosphaeridium scitulum* or *T. erinaceoides* both of which are present in the Rollrock Section (Ingrams *et al.* 2021). *T. erinaceoides* peaks in frequency within three intervals in the Rollrock Section (306.0–312.0 m, 363.0–364.5 m, and 379.5–405.0 m). Species of the genus *Exochosphaeridium* have previously been associated with nearshore, high-energy conditions (Li & Habib 1996; Lamolda & Mao 1999; Harris & Tocher 2003; Barroso-Barcenilla *et al.* 2011; Peyrot *et al.* 2011; van Helmond *et al.* 2014; Carvalho *et al.* 2016).

Species distribution within modern dinoflagellate communities is primarily dependent on a combination of physical and chemical parameters, including turbulence, solar irradiance and nutrient levels (Smayda & Reynolds 2003). Shallow-water and seasonal-bloom species are characteristically small with a high surface area to volume ratio (Smayda & Reynolds 2003). While this does not necessarily influence the morphological characteristics of a cyst, it is notable. For a dinoflagellate, the easiest way to obtain a higher cyst surface area to volume ratio is to produce numerous short spines. This higher surface area to volume ratio prevents cysts from excess movement in high-energy conditions, thereby preventing damage to the theca inside.

6. Summary

A multivariate statistical analysis of the marine palynomorphs recovered from the Late Jurassic to earliest Cretaceous interval of the Rollrock Section, Arctic Canada, allowed for the identification of three clusters and six sub-clusters, each with their own unique floral assemblage. These clusters reflect discrete chronological periods and ecological conditions, which correspond to the stratigraphy of the section. The Oxfordian to Tithonian Ringnes Formation is recorded as being dominated by cluster 1, an assemblage comprising proximate dinoflagellate cysts. The Tithonian to Valanginian Deer Bay Formation is divided by an intra-Berriasian unconformity and is separated into three local assemblage zones based on dinoflagellate cysts with distinct process morphologies. Proximate cysts (cluster 2a) dominate in the Tithonian to lower Berriasian, proximochorate cysts (cluster 2b) in the upper Berriasian, and chorate cysts (cluster 3) in the Valanginian.

Statistical palynological data, combined with sedimentological evidence, subdivides the Rollrock Section into three complete and two incomplete third order stratigraphic sequences. By combining dense and systematic sampling with the analysis of changes in dinoflagellate cyst diversity, distinct fourth order sequences have been recorded across the Jurassic–Cretaceous transition within the Sverdrup Basin for the first time. By analysing multivariate data through this sequence stratigraphic framework, a more complicated environmental transition is observed than previously suggested for the basin, as palynological assemblages are driven by these fourth order cycles.

In the Sverdrup Basin, two groups of dinoflagellate cysts, characterised by process morphology, are observed to act as

environmental proxies that depart from normal conditions. This is evident within fourth order sequences, with proximochorate genera, such as *Lanterna* and *Gochteodinia*, and proximate genera, such as *Pareodinia*, being prevalent during transgressive systems tracts. In contrast, chorate species, such as *O. complex* and *Oligosphaeridium asterigium*, are prevalent during highstands.

The ratio of Rb/Sr, used as a proxy for weathering, coastline proximity, and chemical leaching, is observed to have a direct correlation to palynoassemblage constitution. Elevated Rb/Sr ratios are interpreted to correspond to high-energy, turbid, proximal, and nutrient-rich conditions. These conditions selected for high frequencies of proximochorate cyst bearing dinoflagellates, which were able to outcompete dinoflagellates with other cyst types in regressional tracts.

The ratio of Al/Si is a reliable indicator of clay content in samples, which in turn can be utilised as a proxy for hydrodynamic energy, shoreline proximity, and nutrient availability. A high ratio indicates lower energy, a distal setting and decreased nutrient content, while a low ratio indicates the opposite. In the Rollrock Section, this ratio has a positive correlation with the abundance of chorate cysts; high values of both categories correspond to fourth order transgressional systems tracts.

Integration of these newly discovered fourth order sequences into future palaeoclimate studies, within the Sverdrup Basin and the wider Arctic region, will enable more accurate data to be obtained. Sparse sampling of sections across the Jurassic–Cretaceous transition, which bypasses identification of these cycles, inevitably leads to oversimplifying the environmental perturbations that characterise this interval.

7. Supplementary material

Supplementary material is available online at https://doi.org/10.1017/S1755691022000081.

8. Acknowledgements

9. References

Armentrout, J. M. 1996. High resolution sequence biostratigraphy: examples from the Gulf of Mexico Plio-Pleistocene. *Geological Society, London, Special Publications* **104**, 65–86.

Balkwill, H. R. 1978. Evolution of Sverdrup Basin, Arctic Canada. *American Association of Petroleum Geologists, Bulletin* **62**, 1004–28.

Balkwill, H. R. 1983. Geology of Amund Ringnes, Cornwall and Haig-Thomas islands, District of Franklin. *Geological Survey of Canada, Memoir* **390**, 1–76.

Barroso-Barcenilla, F., Pascual, A., Peyrot, D. & Rodríguez-Lázaro, J. 2011. Integrated biostratigraphy and chemostratigraphy of the upper Cenomanian and lower Turonian succession in Puentedey, Iberian Trough, Spain. *Proceedings of the Geologists' Association* **122**, 67–81.

Calvert, S. E. & Pedersen, T. F. 2007. Chapter fourteen elemental proxies for palaeoclimatic and palaeoceanographic variability in marine sediments: interpretation and application. *Developments in Marine Geology* **1**, 567–644.

Carvalho, M. D. A., Bengtson, P. & Lana, C. C. 2016. Late Aptian (Cretaceous) paleoceanography of the South Atlantic Ocean inferred from dinocyst communities of the Sergipe Basin, Brazil. *Paleoceanography* **31**, 2–26.

Daly, R. J., Jolley, D. W., Spicer, R. A. & Ahlberg, A. 2011. A palynological study of an extinct Arctic ecosystem from the Palaeocene of Northern Alaska. *Review of Palaeobotany and Palynology* **166**, 107–16.

Davies, E. H. 1983. The dinoflagellate Oppel-zonation of the Jurassic–Lower Cretaceous sequence in the Sverdrup Basin, arctic Canada. *Geological Survey of Canada, Bulletin* **359**, 1–59.

Davies, S. J., Lamb, H. F. & Roberts, S. J. 2015. Micro-XRF core scanning in palaeolimnology: recent developments. In Croudace, I. W. & Rothwell, R. G. (eds) *Micro-XRF Studies of Sediment Cores*, 189–226. Dordrecht, Netherlands: Springer.

Dypvik, H. & Harris, N. B. 2001. Geochemical facies analysis of fine-grained siliciclastics using Th/U, Zr/Rb and (Zr + Rb)/Sr ratios. *Chemical Geology* **181**, 131–46.

Embry, A. 2011. Petroleum prospectivity of the Triassic–Jurassic succession of Sverdrup Basin, Canadian Arctic Archipelago. *Geological Society, London, Memoirs* **35**, 545–58.

Embry, A. F. 1985. New stratigraphic units, Middle Jurassic to lowermost Cretaceous succession, Arctic Islands. *Geological Survey of Canada, Paper* **85-1B**, 269–76.

Embry, A. F. 1993. Transgressive–regressive (T-R) sequence analysis of the Jurassic succession of the Sverdrup Basin, Canadian Arctic Archipelago. *Canadian Journal of Earth Sciences* **30**, 301–20.

Embry, A., Beauchamp, B., Dewing, K., Dixon, J., Piepjohn, K., Strauss, J. V., Reinhardt, L. & McClelland, W. C. 2019. Episodic tectonics in the Phanerozoic succession of the Canadian High Arctic and the "10-million-year flood". Circum-Arctic structural events: tectonic evolution of the Arctic margins and Trans-Arctic links with adjacent orogens. Edited by K. Piepjohn, JV Strauss, L. Rein hardt, L., and WC McClelland. Geological Society of America Special Paper, 541, 213–30.

Embry, A. F. & Beauchamp, B. 2019. Chapter 14. Sverdrup basin. In Miall, A. D. (ed.) *The sedimentary basins of the United States and Canada*, 2nd ed., 559–92. New York: Elsevier.

Galeotti, S., Brinkhuis, H. & Huber, M. 2004. Records of post–Cretaceous-Tertiary boundary millennial-scale cooling from the western Tethys: a smoking gun for the impact-winter hypothesis? *Geology* **32**, 529–32.

Galloway, J. M., Sweet, A. R., Swindles, G. T., Dewing, K., Hadlari, T., Embry, A. F. & Sanei, H. 2013. Middle Jurassic to Lower Cretaceous paleoclimate of Sverdrup Basin, Canadian Arctic Archipelago inferred from the palynostratigraphy. *Marine and Petroleum Geology* **44**, 240–55.

Galloway, J. M., Tullius, D. N., Evenchick, C. A., Swindles, G. T., Hadlari, T. & Embry, A. F. 2015. Early Cretaceous vegetation and climate change at high latitude: palynological evidence from Isachsen Formation, Arctic Canada. *Cretaceous Research* **56**, 399–420.

Galloway, J. M., Vickers, M., Price, G. D., Poulton, T. P., Grasby, S. E., Hadlari, T., Beauchamp, B. & Sulphur, K. 2020. Finding the VOICE: organic carbon isotope chemostratigraphy of the Late Jurassic–Early Cretaceous of Arctic Canada. *Geological Magazine* **157**, 1643–1657.

Hadlari, T., Midwinter, D., Galloway, J. M., Dewing, K. & Durbano, A. M. 2016. Mesozoic rift to post-rift tectonostratigraphy of the Sverdrup Basin, Canadian Arctic. *Marine and Petroleum Geology* **76**, 148–58.

Hammer, Ø., Harper, D. A. T. & Ryan, P. D. 2001. PAST: paleontological statistics software package for education and data analysis. *Palaeontologia Electronica* **4**, 9pp.

Hammer, Ø. & Harper, D. A. T. 2006. *Paleontological data analysis*. Chichester: Blackwell.

Haq, B. U. 2014. Cretaceous eustasy revisited. *Global and Planetary Change* **113**, 44–58.

Harris, A. J. & Tocher, B. A. 2003. Palaeoenvironmental analysis of Late Cretaceous dinoflagellate cyst assemblages using high-resolution sample correlation from the Western Interior Basin, USA. *Marine Micropaleontology* **48**, 127–48.

Harrison, J. C., St-Onge, M. R., Petrov, O. V., Strelnikov, S. I., Lopatin, B. G., Wilson, F. H., Tella, S., Paul, D., Lynds, T., Shokalsky, S. P., Hults, C. K., Bergman, S., Jepsen, Numerical H. F. & Solli, A. 2011. Geological map of the Arctic. *Geological Survey of Canada. Map*, 2159A.

Hill, M. O. 1979. *DECORANA — A FORTRAN program for detrended correspondence analysis and reciprocal averaging*. Section of Ecology and Systematics, Cornell University.

Hill, M. O. & Gauch, H. G. 1980. Detrended correspondence analysis: an improved ordination technique. *Vegetatio* **42**, 47–58.

Ingrams, S., Jolley, D. W. & Schneider, S. 2021. High latitude stratigraphical palynology of the Jurassic–Cretaceous boundary interval, Sverdrup Basin, Arctic Canada. *Cretaceous Research* **126**, 104922.

Jelby, M. E., Śliwińska, K. K., Koevoets, M. J., Alsen, P., Vickers, M. L., Olaussen, S. & Stemmerik, L. 2020. Arctic Reappraisal of global carbon-cycle dynamics across the Jurassic–Cretaceous boundary and Valanginian Weissert event. *Palaeogeography, Palaeoclimatology, Palaeoecology* **555**, 109847.

Jeletzky, J. A. 1984. Jurassic – cretaceous boundary beds of western and Arctic Canada and the problem of the Tithonian–Berrisian stages in the Boreal Realm. In: Westermann, G.E.G. Jurassic–Cretaceous biochronology and biogeography of North America. *Geological Association of Canada, Special paper* **27**, 175–255.

Kemper, E. 1975. Upper Deer Bay Formation (Berriasian–Valanginian) of Sverdrup Basin and biostratigraphy of the Arctic Valanginian. *Geological Survey of Canada, Paper* **75–1B**, 45–54.

Kovach, W. L. 1993. Multivariate techniques for biostratigraphical correlation. *Journal of the Geological Society, London* **150**, 697–705.

Lamolda, M. A. & Mao, S. 1999. The Cenomanian–Turonian boundary event and dinocyst record at Ganuza (northern Spain). *Palaeogeography, Palaeoclimatology, Palaeoecology* **150**, 65–82.

Lebedeva, N. K. & Nikitenko, B. L. 1999. Dinoflagellate cysts and microforaminifera of the Lower Cretaceous Yatria River section, Subarctic Ural, NW Siberia (Russia). Biostratigraphy, palaeoenvironmental and palaeogeographic discussion. *Grana* **38**, 134–43.

Lentin, J. K. & Williams, G. L. 1980. Dinoflagellate provincialism with emphasis on *Campanian peridiniaceans. American Association of Stratigraphic Palynologists, Contributions Series* **no. 7**, 1–47.

Li, H. & Habib, D. 1996. Dinoflagellate stratigraphy and its response to sea level change in Cenomanian–Turonian sections of the Western Interior of the United States. *Palaios* **11**, 15–30.

Mayr, U. & Trettin, H. P. 1996. Geology, Tanquary Fiord, District of Franklin, Northwest Territories. *Geological Survey of Canada. Map* 1886A, scale 1:250,000.

Mertens, K. N., Bradley, L. R., Takano, Y., Mudie, P. J., Marret, F., Aksu, A. E., Hiscott, R. N., Verleye, T. J., Mousing, E. A., Smyrnova, L. L. & Bagheri, S. 2012a. Quantitative estimation of Holocene surface salinity variation in the Black Sea using dinoflagellate cyst process length. *Quaternary Science Reviews* **39**, 45–59.

Mertens, K. N., Bringué, M., Van Nieuwenhove, N., Takano, Y., Pospelova, V., Rochon, A., De Vernal, A., Radi, T., Dale, B., Patterson, R. T. & Weckström, K. 2012b. Process length variation of the cyst of the dinoflagellate *Protoceratium reticulatum* in the North Pacific and Baltic-Skagerrak region: calibration as an annual density proxy and first evidence of pseudo-cryptic speciation. *Journal of Quaternary Science* **27**, 734–44.

Mertens, K. N., Ribeiro, S., Bouimetarhan, I., Caner, H., Nebout, N. C., Dale, B., De Vernal, A., Ellegaard, M., Filipova, M., Godhe, A. & Goubert, E. 2009. Process length variation in cysts of a dinoflagellate, *Lingulodinium machaerophorum*, in surface sediments: investigating its potential as salinity proxy. *Marine Micropaleontology* **70**, 54–69.

Morley, R. J. 1996. Biostratigraphic characterization of systems tracts in Tertiary sedimentary basins. In *Proceedings of the international symposium on sequence stratigraphy, S.E. Asia*, 49–71.

Nguyen, A. V., Galloway, J. M., Poulton, T. P. & Dutchak, A. R. 2020. Calibration of Middle to Upper Jurassic palynostratigraphy with Boreal ammonite zonations in the Canadian Arctic. *Bulletin of Canadian Petroleum Geology* **68**, 65–90.

Nichols, G. 2009. *Sedimentology and stratigraphy*. Chichester: John Wiley & Sons.

Nøhr-Hansen, H., Piasecki, S. & Alsen, P. 2019. A Cretaceous dinoflagellate cyst zonation for NE Greenland. *Geological Magazine* **157**, 1658–92.

Paliy, O. & Shankar, V. 2016. Application of multivariate statistical techniques in microbial ecology. *Molecular Ecology* **25**, 1032–57.

Peyrot, D., Barroso-Barcenilla, F., Barrón, E. & Comas-Rengifo, M. J. 2011. Palaeoenvironmental analysis of Cenomanian–Turonian dinocyst assemblages from the Castilian Platform (northern-Central Spain). *Cretaceous Research* **32**, 504–26.

Pocock, S. A. J. 1976. A preliminary dinoflagellate zonation of the uppermost Jurassic and lower part of the Cretaceous, Canadian Arctic, and possible correlation in the western Canada Basin. *Geoscience and Man* **15**, 101–14.

Posamentier, H. W., Jeniey, M. T. Vail, P. R. 1988. Eustatic controls on clastic deposition 1 conceptual framework. In Wilgus, C. K., Hastings, B. S., Kendall, C. G. St. C., Posamentier, H. W., Ross, C. A. & van Wagoner, J. C. (eds) *Sea level changes – An integrated approach*, 109–124. Tulsa, Oklahoma: SEPM Special Publication **42**.

Poulsen, N. E. & Riding, J. B. 2003. The Jurassic dinoflagellate cyst zonation of subboreal Northwest Europe. *Geological Survey of Denmark and Greenland (GEUS) Bulletin* **1**, 115–44.

Ramette, A. 2007. Multivariate analyses in microbial ecology. *FEMS Microbiology Ecology* **62**, 142–60.

Retallack, G. J. 2008. *Soils of the past: an introduction to paleopedology*. Chichester: John Wiley & Sons.

Reynolds, C. S. 1989. Physical determinants of phytoplankton succession. In Sommer, U. (ed.) *Plankton ecology*, 9–56. Berlin, Heidelberg: Springer.

Sarjeant, W. A. S. 1982. Dinoflagellate cyst terminology: a discussion and proposals. *Canadian Journal of Botany* **60**, 922–45.

Schneider, S., Kelly, S. R. A., Mutterlose, J., Herrle, J. O., Hülse, P., Jolley, D. W., Schröder-Adams, C. J. & Lopez-Mir, B. 2020. Macrofauna and biostratigraphy of the Rollrock Section, northern Ellesmere Island, Canadian Arctic Islands – a comprehensive high latitude archive of the Jurassic–Cretaceous transition. *Cretaceous Research* **114**, 104508.

Sliwinska, K. K., Jelby, M. E., Grundvåg, S. A., Nøhr-Hansen, H., Alsen, P. & Olaussen, S. 2020. Dinocyst stratigraphy of the ValanginianeAptian Rurikfjellet and Helvetiafjellet formations on Spitsbergen, Arctic Norway. *Geological Magazine* **157**, 1693–714.

Smayda, T. J. 2002. Adaptive ecology, growth strategies and the global bloom expansion of dinoflagellates. *Journal of Oceanography* **58**, 281–94.

Smayda, T. J. & Reynolds, C. S. 2001. Community assembly in marine phytoplankton: application of recent models to harmful dinoflagellate blooms. *Journal of Plankton Research* **23**, 447–61.

Smayda, T. J. & Reynolds, C. S. 2003. Strategies of marine dinoflagellate survival and some rules of assembly. *Journal of Sea Research* **49**, 95–106.

Tennant, J. P., Mannion, P. D., Upchurch, P., Sutton, M. D. & Price, G. D. 2017. Biotic and environmental dynamics through the Late Jurassic–Early Cretaceous transition: evidence for protracted faunal and ecological turnover. *Biological Reviews* **92**, 776–814.

Ter Braak, C. J. F. 1986. Canonical correspondence analysis: a new eigenvector technique for multivariate direct gradient analysis. *Ecology* **67**, 1167–79.

van Helmond, N. A. G. M., Sluijs, A., Damsté, J. S., Reichart, G. J., Voigt, S., Erbacher, J., Pross, J. & Brinkhuis, H. 2014. Freshwater discharge controlled deposition of Cenomanian–Turonian black shales on the NW European epicontinental shelf (Wunstorf, North Germany). *Climate of the Past* **10**, 3755–86.

van Wagoner, J. C., Posamentier, H. W., Mitchum, R. M. J., Vail, P. R., Sarg, J. F., Loutit, T. S. & Hardenbol, J. 1988. An overview of the fundamentals of sequence stratigraphy and key definitions. In Wilgus, C. K., Hastings, B. S., Kendall, C. G. St. C., Posamentier, H. W., Ross, C. A. & van Wagoner, J. C. (eds) *Sea level changes: an integrated approach*, 39–45. Special Pyblication 42, Tulsa, OK: Society of Economic Paleontologists and Mineralogists.

Wilson, D. G. 1976. Studies of Mesozoic stratigraphy, Tanquary Fiord to Yelverton Pass, northern Ellesmere Island, District of Franklin. *Geological Survey of Canada, Paper* **76–1A**, 449–51.

Wornardt, W.W., 1993 *Sequence stratigraphy concepts and applications*. Micro-Strat. Inc. (Wall Chart, version 2.0).